

CaCu_2O_8 .² These layered compounds have double bismuth oxide layers in which the Bi lone pairs are oriented between the two BiO sheets thus imparting a micaceous morphology.

(16) Johnson, C. K. ORTEP: *A Fortran Thermal-Ellipsoid Plot Program for Crystal Structure Illustration*; Oak Ridge National Laboratory Report 5138, 1976.

Acknowledgment. The technical assistance of W. J. Marshall for the X-ray data collection, C. R. Miao for syntheses, and M. A. Saltzberg and S. C. Winchester for DSC measurements is acknowledged.

Supplementary Material Available: A listing of structure factor amplitudes (5 pages). Ordering information is given on any current masthead page.

Luminescence Efficiency of Ions with Broad-Band Excitation in Lithium Lanthanum Phosphate Glass

J. W. M. Verwey* and G. Blasse

Debye Research Institute, University of Utrecht, P.O. Box 80,000, 3508 TA Utrecht, The Netherlands

Received March 12, 1990

The luminescence of several ions in lithium lanthanum phosphate glass is investigated and compared with the luminescence of these ions in lanthanum borate glass. The efficiency of the luminescence is much higher in the phosphate glass. For some ions a comparison with their luminescence in crystalline $\text{LiLaP}_4\text{O}_{12}$ is also made. The results lead to some conclusions about the influence of the host material on the luminescence efficiency. These results are discussed, and examples are used to illustrate these conclusions.

Introduction

In a previous paper the authors reported the luminescence efficiency of several ions in lanthanum borate (LaB_3O_6) glass and in crystalline LaB_3O_6 .¹ The luminescence efficiency for excitation into broad bands was much lower in the glass than in the crystals. A single configurational coordinate (scc) model was used to explain the different luminescence efficiencies of these ions in both modifications. However, the trends and rules noted in that study were proven valid only for the crystalline borate and glass modifications, so it seemed worthwhile to investigate whether they are also valid in a different host. Lithium lanthanum phosphate ($\text{LiLaP}_4\text{O}_{12}$) is a logical choice due to the following reasons: (a) The crystalline material has been studied intensively because of its possibilities as a stoichiometry laser material;^{2,3} (b) efficient broad-band luminescence has been reported for several activators in the crystalline modification;⁴ (c) phosphate glasses are investigated and used for high average power (hap) lasers;⁵ (d) to our knowledge, there has been only one comparison of the luminescence in the glassy and crystalline modifications for Nd^{3+} - Yb^{3+} energy transfer in $\text{LiLaP}_4\text{O}_{12}$.⁶ Only the narrow $4f^n$ transitions were studied here.

In this paper we report a luminescence investigation of several ions with broad-band excitation transitions in lithium lanthanum phosphate crystals and glasses. The luminescence efficiency is, generally speaking, higher than that for the borate glass. By examining the differences in the spectra, we are able to determine the influence of the nature of the host material on the luminescence of the ions. It will be shown that by using the scc model, it is possible

to predict qualitatively the luminescence efficiency of doped glasses.

Experimental Section

Preparation. The starting materials for the preparation of the lithium lanthanum phosphate (LLP) glasses are $\text{NH}_4\text{H}_2\text{PO}_4$, Cr_2O_3 , and Li_2CO_3 (Merck p.a.), Bi_2O_3 (Baker), and the rare-earth oxides La_2O_3 , CeO_2 , Pr_4O_{11} , Eu_2O_3 , Gd_2O_3 , and Tb_2O_7 (Highways International, 5N). The dopant concentration is ~ 1 mol %. Due to the volatility of phosphorus pentoxide, an excess of 10–12% $\text{NH}_4\text{H}_2\text{PO}_4$ was added to the stoichiometric mixture before melting. This mixture is heated for 2 h at 250 °C and 3 h at 550 °C. When most of the H_2O and NH_3 have been evaporated, the mixture is melted in a quartz crucible at 1270 °C for ~ 30 min. The glasses containing Ce^{3+} , Pr^{3+} , or Tb^{3+} are melted under a N_2/H_2 mixture (4:1). The glasses are poured into a carbon mould at 470 °C and cooled to room temperature at a rate of 1 °C/min. Crystalline samples of composition $\text{LiLa}_{1-x}\text{M}_x\text{P}_4\text{O}_{12}$ ($\text{M} = \text{Ce}^{3+}$, Eu^{3+} , Tb^{3+} , Bi^{3+}) are prepared according to the literature.^{4,7,8} They are checked by X-ray powder diffraction and infrared spectroscopy.⁸ The results show these samples to be single phase.

Optical Measurements. Luminescence spectra were measured on powdered samples and on polished glass samples of $6 \times 6 \times 10$ mm. Measurements were carried out at various temperatures ranging from 4.2 to 300 K. Emission and excitation spectra were recorded with a Perkin-Elmer MPF 3L spectrophotometer equipped with an Oxford Instruments helium flow cryostat. The spectra were corrected for the lamp intensity and the transmittance of the monochromator with the use of Lumogen T-rot G.G as a standard.⁹ For excitation wavelengths shorter than 240 nm, the setup described in ref 10 was used. Diffuse reflection spectra of the powdered samples were recorded at room temperature with a Perkin-Elmer Lambda 7 UV/vis spectrophotometer. The same apparatus was used to measure the absorption spectra of 6-mm-thick glass samples. The absorption spectra were not corrected for reflectance losses. The luminescence efficiency is determined by comparison with standard phosphors.

(1) Verwey, J. W. M.; Blasse, G. *Mater. Chem. Phys.* 1990, 25, 91.

(2) Krühler, W. W.; Jeser, J. P.; Danielmeyer, H. G. *Appl. Phys.* 1973, 2, 329.

(3) Danielmeyer, H. G.; Weber, H. P. *IEEE J. Quantum Electron.* 1973, QE-8, 805.

(4) Blasse, G.; Dirksen, G. J. *Phys. Status Solidi B* 1982, 110, 487.

(5) Marion, J. E. Advanced phosphate glasses for high-average-power lasers, Glasses for Optoelectronics. *Proc. SPIE* 1989, 1128, 318.

(6) Parent, C.; Lurin, C.; LeFlem, G.; Hagenmuller, P. *J. Lumin.* 1986, 36, 49.

(7) Moktar, M. F.; Ariguib, N. K.; Trabelsi, M. *J. Solid State Chem.* 1981, 38, 128.

(8) Rzaigni, M.; Ariguib, N. K. *J. Solid State Chem.* 1981, 39, 128.

(9) Bril, A.; de Jager-Veenis, A. W. *J. Res. NBS* 1976, 80A, 401.

(10) Verwey, J. W. M.; Dirksen, G. J.; Blasse, G. *J. Non-Crystalline Solids* 1988, 107, 49.

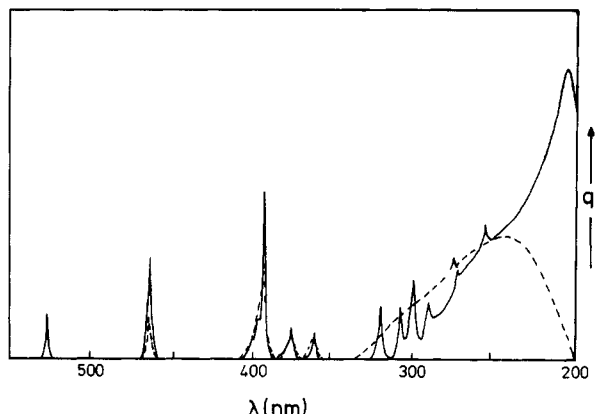


Figure 1. Excitation spectrum of the $5D_0$ emission of Eu^{3+} in LLP glass (solid line) and in borate glass (broken line) at 4.2 K. The intensity of the $7F_0 \rightarrow 5D_1$ transition at 525 nm is set equal in these spectra. q_r gives the relative quantum output in arbitrary units.

Table I. Quantum Efficiency q_{cts} of the Eu^{3+} Emission for CTS Excitation in Different Hosts

q_{cts} , %	temp, K	host	ref
~10	300	LaB_3O_6 glass	1
~10	4.2	LaB_3O_6 glass	1
high	300	LaB_3O_6 crystal	1
high	4.2	LaB_3O_6 crystal	1
~20	300	LLP glass	this work
~35	4.2	LLP glass	this work
high	300	LLP crystal	this work
high	4.2	LLP crystal	this work

For the decay time measurements, a setup was used that consisted of a Molelectron DL-200 dye laser, pumped with a Molelectron UV 14 N₂ laser, in combination with a Spex 1-m monochromator and a Thor bath cryostate. A multichannel analyzer with a minimum time scale of 10 μs was used to record the time dependence of the luminescence.

Results

Charge-Transfer Excitation of the Eu^{3+} Ion. The Eu^{3+} ion was studied because the charge-transfer state (CTS) of this ion is very sensitive to changes in the surroundings of the ion, whereas the intensity of the $7F_0 \rightarrow 5D_1$ magnetic dipole transition does not depend on the surroundings. This makes it easy to compare the Eu^{3+} luminescence efficiency of the glasses and crystals with commercial phosphors for which the efficiency has been accurately determined.

Figure 1 shows the excitation spectra of the Eu^{3+} luminescence in LLP glass and in lanthanum borate glass at 4.2 K. The spectra have been normalized with the intensity of the $7F_0 \rightarrow 5D_1$ excitation transition, as this intensity is independent of the surroundings. Two differences can be observed: (a) the maximum of the CTS in LLP glass is situated at a higher energy than that of the CTS in the lanthanum borate glass; (b) the maximum intensity of the CTS in the lanthanum borate glass is less than 50% of the CTS intensity in the LLP glass. The charge-transfer excitation band ranges from 345 to around 205 nm in the lanthanum borate glass, while for the LLP glass it ranges from 275 to shorter than 200 nm. These results for the LLP glass are in accordance with the earlier studies on Eu^{3+} in phosphate glasses.^{11,12}

Table I shows the estimated quantum efficiencies (q) for charge-transfer excitation of the Eu^{3+} luminescence in

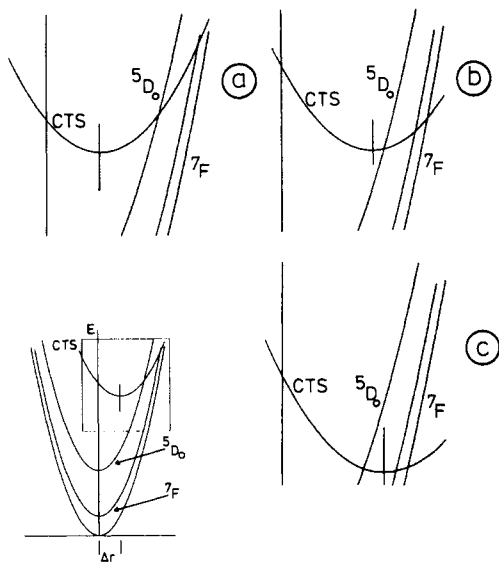


Figure 2. Configuration coordinate models of (a) Eu^{3+} in the crystalline modifications, (b) Eu^{3+} in LLP glass, and (c) Eu^{3+} in a borate glass. See also text.

Table II. Dependence of the Decay Time of Eu^{3+} Luminescence on the Position of the Charge-Transfer Excitation Band in a Number of Glasses

	glass				
	LLP	GdB_3O_6	LaB_3O_6	GdBGeO_5	LaBGeO_5
$\tau_{300\text{ K}}, \text{ms}$	2.6	2.0	1.9	1.5	1.5
$\tau_{4.2\text{ K}}, \text{ms}$	3.3	2.2	2.0	1.8	1.7
τ_r , ^a ms	2.9 ^b	2.7	2.7	2.5	2.5
max CT exc	204	245	250	255	265
band, nm					
onset CT exc	275	340	345	345	345
band, nm					

^a Calculated from eq 1. ^b τ_r of Eu^{3+} in the LLP glass is temperature dependent and decreases from 3.1 ms at 4.2 K to 2.9 ms at 300 K.

the LLP and borate hosts in both the glass and the crystalline modifications. At both 4.2 K and room temperature, the value of q is high in the crystals of LLP and LaB_3O_6 . In the LLP glass it is 20%, and in the borate glass it is 10–15% at room temperature. At lower temperatures this efficiency does not improve for the borate glass, but for the LLP glass q increases up to about 35% at 4.2 K. To our knowledge, this is the highest q_{cts} for Eu^{3+} in a glass that has been observed. Though this q_{cts} is high for a glass, the q_{cts} for the $\text{LiLaP}_4\text{O}_{12}$ crystals is much higher. This is in accordance with the results in ref 1.

From these results we derive the single-configuration coordinate (SCC) models shown in Figure 2. Here we use the conclusion arrived at in ref 1 that the parabola offset in glasses is larger than that in crystals. Figure 2a shows the SCC model for Eu^{3+} in the crystalline modification, the offset of the CTS parabola (Δr) is so small that the CTS does not feed the $7F$ ground multiplet. Only the $5D$ and higher multiplets are populated. This results in an efficient luminescence after CTS excitation at room temperature and below. Figure 2b shows the SCC model of Eu^{3+} in LLP glass: the value of Δr is larger. Depending on the exact value of Δr , both $7F$ and $5D$ multiplets are populated, i.e., the quantum efficiency will become smaller than 1. While Figure 2b implies a temperature-dependent value of q , with the transition CTS $\rightarrow 7F$ containing an energy barrier, Figure 2c shows a situation where the temperature dependence vanishes (as in the borate glass). Even at 4.2 K, the CTS empties for the greater part into the $7F$ multiplet

(11) Reisfeld, R.; Lieblich, N. *J. Phys. Chem. Solids* 1967, 34, 1467.

(12) Reisfeld, R.; Eckstein, Y. *J. Chem. Phys.* 1975, 63, 4001.

by tunneling so that q becomes very low.

To prove that the nonradiative loss occurs via the CTS and not within the $4f^6$ configuration, the decay time of the Eu^{3+} ion was studied, and the results are presented in Table II. All decay curves are single exponential. The long decay time of the Eu^{3+} emission of europium-doped LLP glass (about 3 ms) shows that the nonradiative losses within the $4f^6$ configuration are insignificant. This result confirms the model proposed above. To substantiate this, the radiative decay time was calculated. Since the radiative transition probability of the $^5D_0 \rightarrow ^7F_1$ magnetic dipole emission transition ($P_{\text{md}} = 50 \text{ s}^{-1}$)¹³ is independent of the surroundings of the Eu^{3+} ion, it is possible to calculate the radiative decay rate (τ_r) of the 5D_0 level from the total emission intensity (I_{tot}) and the magnetic dipole emission intensity (I_{md}).¹⁴ The corresponding expression is

$$\tau_r = I_{\text{md}} / (P_{\text{md}} I_{\text{tot}}) \quad (1)$$

Thus we obtain $\tau_r = 2.9 \text{ ms}$, which is in excellent agreement with the experimental value in spite of the rough calculation. This proves that the nonradiative loss occurs from the CTS.

However, this model cannot account for the temperature dependence of the experimental decay time. To investigate this and to determine whether the good agreement between the experimental and calculated decay times is general, we also measured decay times in a number of other europium-doped glasses. The results are given in Table II, along with the calculated τ_r values and the position of the CTS absorption band.

Table II shows three clear trends: (a) If the CTS is situated at a longer wavelength, i.e., at a lower energy, the decay time becomes shorter. (b) The agreement between the calculated value τ_r and the experimental values of the decay time becomes less satisfactory if the CTS shifts to lower energy. (c) The temperature dependence of the experimental decay rates is more pronounced if the CTS is situated at high energy. This is emphasized by the case of LLP: at 4.2 K this decay time is 3.3 ms, while at room temperature it is 2.6 ms. For the other glasses this temperature dependence is much weaker. The calculated τ_r values are temperature independent for all glasses except for LLP:Eu³⁺. Here $\tau_r = 3.1 \text{ ms}$ at 4.2 K and 2.9 ms at 300 K. This change is much smaller than that in the experimental values.

The discrepancy between the experimental and calculated values of the decay time is especially startling, since they seem to suggest nonradiative losses within the $4f^6$ configuration. Let us consider this possibility in more detail.

First, we consider multiphonon emission between the emitting 5D_0 level and the 7F_6 level. The nonradiative rate for this process can be estimated by using the modified energy gap law.¹⁵ The nonradiative rate is given by

$$K_{\text{nr}}(T) = K_{\text{nr}}(0)(n + 1)^p \quad (2)$$

where $K_{\text{nr}}(T)$ is the rate at temperature T , $p = \Delta E / \hbar \omega$, ΔE is the energy difference between the levels involved

$$n = [\exp(\hbar \omega / kT) - 1]^{-1} \quad (3)$$

$$K_{\text{nr}}(0) = \beta \exp[-(\Delta E - 2\hbar \omega_{\text{max}})\alpha] \quad (4)$$

and α and β are known constants, for borate glasses $4.3 \times 10^{-3} \text{ cm}$ and $16.8 \times 10^7 \text{ s}^{-1}$, respectively. ω_{max} is the highest available vibrational frequency ($\sim 1400 \text{ cm}^{-1}$).¹⁶

(13) Ofelt, G. S. *J. Chem. Phys.* 1962, 37, 511.

(14) Blasse, G.; Bril, A. *Philips Res. Rep.* 1967, 22, 481.

(15) van Dijk, J. M. F.; Schuurmans, M. F. *J. Chem. Phys.* 1983, 78, 5317.

Table III. Representations of the J Levels of Eu^{3+} under C_s Symmetry

J	representation	selection rules for the transitions $^5D_0 \rightarrow ^7F_J$
0	A'	ED allowed
1	$A' + 2A''$	MD and ED allowed (3 \times)
2	$3A' + 2A''$	ED allowed (5 \times)

The calculated nonradiative rate is $2.6 \times 10^{-9} \text{ s}^{-1}$ at 300 K. Since the radiative rate is of the order of $3 \times 10^2 \text{ s}^{-1}$, nonradiative losses due to multiphonon emission can be neglected.

Second, we consider the possibility of thermal excitation from the 5D_0 level to the CTS from which nonradiative decay will follow. The problem is to estimate the energy difference between the equilibrium state of the CTS and the 5D_0 level. Since the onset of the CTS absorption band is at about 28000 cm^{-1} and the 5D_0 level is at about 17300 cm^{-1} , a value of 10000 cm^{-1} seems to be a good estimation for the energy difference. Further we take 10^{13} s^{-1} to be the nonradiative rate of the CTS.¹⁷ This brings the nonradiative rate from 5D_0 via the CTS to the ground state at 300 K to $10^{13} \exp(-10000/200) \sim 1.9 \times 10^{-8} \text{ s}^{-1}$. This value is also much too small to compete with the radiative rate. At 4.2 K this is even more true.

Since it is hard to consider other nonradiative processes of any importance, we conclude that the calculated value of τ_r is incorrect, i.e., the value of the radiative rate of the total $^5D_0 \rightarrow ^7F_1$ transition depends on the surroundings of the Eu^{3+} ion. Although this transition is forbidden as a forced electric-dipole transition,^{13,18} it can nevertheless obtain some electric-dipole intensity by J - J mixing. This is most easily illustrated as follows.

Let us assume the site symmetry of Eu^{3+} in the glasses is C_s , as is usually considered to be the case.^{19,20} The representations of the J levels under this symmetry and the selection rules for transitions between them are given in Table III. This shows that the levels of the $J = 2$ level can mix with the similar ones of $J = 1$, i.e., the $^5D_0 \rightarrow ^7F_1$ emission will acquire a certain electric-dipole character next to its magnetic-dipole character. It is well-known that for a given symmetry the intensity of the ED lines and especially those of the $^5D_0 \rightarrow ^7F_{0,2}$ transitions increases strongly if the CTS shifts to lower energy.^{21,22} Due to J - J mixing, the $^5D_0 \rightarrow ^7F_1$ radiative rate will also increase, stealing a little transition probability from $^5D_0 \rightarrow ^7F_2$. However, in that case the use of eq 1 with $P_{\text{md}} = 50 \text{ s}^{-1}$ is no longer appropriate.

For the borogermanate glass (see Table II), we derive for $P(^5D_0 \rightarrow ^7F_1)$ a value of 75 s^{-1} using an average value of 1.7 ms for the experimental decay time in eq 1. It is interesting that for $\text{YAlO}_3\text{:Eu}^{3+}$ this value is 110 s^{-1} .²³

These considerations explain why the discrepancy between the experimental decay times and τ_r increases for a lower energy position of the CTS. They also show why the experimental decay times decrease in the same sequence since the $^5D_0 \rightarrow ^7F_2$ transition probability increases as the decay time shortens. The temperature dependence is then explained by a thermal shift of the CTS as observed

(16) Schuurmans, M. F.; van Dijk, J. M. F. *Physica* 1984, 123B, 131.

(17) Struck, C. W.; Fonger, W. H. *J. Lumin.* 1970, 12, 456.

(18) Judd, B. R. *Phys. Rev.* 1962, 127, 750.

(19) Reisfeld, R.; Eckstein, Y. *J. Sol. State Chem.* 1972, 5, 1467.

(20) Kandpal, H. C.; Joshi, K. C. *J. Non-Crystalline Solids* 1988, 101, 243.

(21) Blasse, G.; Bril, A. *Philips Res. Rep.* 1966, 21, 368.

(22) Blasse, G.; Bril, A. *J. Chem. Phys.* 1967, 47, 5442.

(23) Weber, M. J.; Varitimis, T. E.; Matsinger, B. H. *Phys. Rev.* 1973, B8, 47.

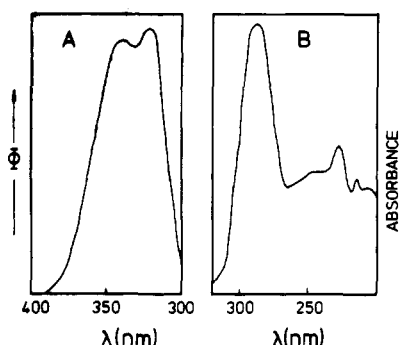


Figure 3. (A) Emission spectrum of Ce^{3+} in LLP glass at 4.2 K. Φ gives the radiant power per constant wavelength interval in arbitrary units. Excitation wavelength is 240 nm. (B) Absorption spectrum of Ce^{3+} in LLP glass at 293 K.

experimentally: for LLP:Eu³⁺ glass its maximum is more than 1000 cm^{-1} shifted to lower energy upon increasing the temperature from 4.2 to 300 K.

In conclusion, the nonradiative losses that occur upon CTS excitation of the Eu³⁺ ion in glasses are exclusively due to the nonradiative transitions from the CTS state.

4f-5d Excitation in Rare-Earth Ions. The ions Ce³⁺, Pr³⁺, and Tb³⁺ were used to study the quantum efficiency upon excitation into the $4f \rightarrow 5d$ transitions of rare-earth ions. Earlier¹ we showed that Δr is much smaller for this transition than that for the CT transition. Upon 4f5d broad-band UV excitation the LLP glasses doped with Ce³⁺, Pr³⁺, and Tb³⁺ show efficient luminescence from these ions. This is now considered in more detail.

Ce³⁺ Ion. The emission spectrum of the Ce³⁺ ion in the LLP glass at 4.2 K consists of a band with two maxima, at 322 and 340 nm (Figure 3A). This emission is due to a $5d \rightarrow 4f$ transition. The absorption spectrum consists of several bands with maxima at 288, 244, 228, and 210 nm (Figure 3B). These are due to $4f \rightarrow 5d$ transitions. The Stokes shift of the Ce³⁺ emission in the LLP glass is $\sim 3600 \text{ cm}^{-1}$, which is less than in the borate glass ($\sim 4700 \text{ cm}^{-1}$). The Stokes shift is proportional to the offset (Δr) of the excited-state parabola. Here we have direct evidence that the offset of broad-band excited states is smaller in the phosphate than in the borate glass. This agrees with our conclusion on the Eu³⁺ luminescence in LLP and borate glasses.

The two maxima in the emission spectrum results from the spin-orbit splitting of the Ce³⁺ ground state ($^2\text{F}_{7/2} - ^2\text{F}_{5/2}$). The splitting obtained from the spectrum in Figure 3A is about 2000 cm^{-1} and agrees with the known value of 2200 cm^{-1} . This splitting was not observed in silicate or borate glasses^{1,24} as the inhomogeneous broadening is larger in these glasses. Such a difference in inhomogeneous broadening was observed before for Cr³⁺ in these glasses.²⁵ The Stokes shift for Ce³⁺ in the crystalline modification of LiLaP₄O₁₂ can be determined only for one Ce³⁺ ion observed in this lattice.⁴ It amounts to 2300 cm^{-1} , which is much smaller than that in the glass. This confirms that the relaxation in the excited state is larger in the glass than it is in the crystal.

The decay time of the Ce³⁺ emission in LLP glass is 35 ns. The decay curve is exponential. This short decay time, which is mainly radiative, reflects the allowed $5d \rightarrow 4f$ transition to which it corresponds. This decay time is shorter than for Ce³⁺ in lanthanum borate glass, which

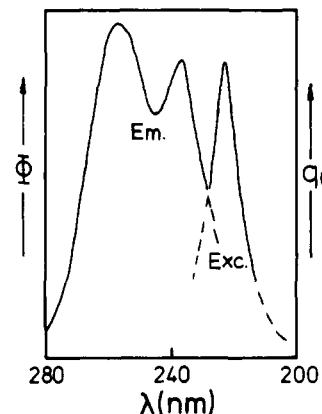


Figure 4. Emission and excitation spectra of the luminescence of Pr^{3+} in LLP glass. The excitation wavelength is 230 nm. The monitored emission wavelength is 270 nm.

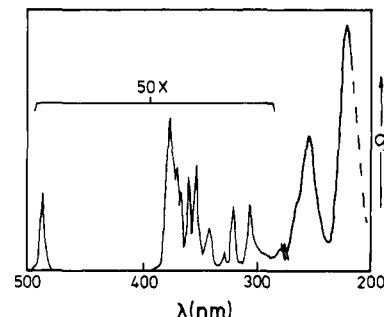


Figure 5. Excitation spectrum of $^5\text{D}_4$ emission of Tb^{3+} in LLP glass at 4.2 K.

amounts to 42 ns. The difference is mainly accounted for by the fact that the radiative transition probability depends on ν^3 (the wavenumber of the maximum of the transition): the ratio $35/42 = 0.83$, whereas the ratio of the emission maxima yields $(331/385)^3 = 0.64$. The agreement is considered to be satisfactory in view of the experimental inaccuracies.

Pr³⁺ Ion. The Pr³⁺ ion in LLP glass shows efficient UV luminescence at room temperature and below. This emission is due to the $4f5d \rightarrow 4f^2$ transition.¹ The maximum of the excitation band is at 221 nm, while the first maximum of the emission band is at 237 nm (Figure 4). The Stokes shift is about 2800 cm^{-1} . This number is not very accurate because the measurement of the excitation spectrum is hampered by the limitations of the instrumental setup, and there is also a strong self-absorbance on the high-energy side of the emission spectrum. Nevertheless, this Stokes shift is much smaller than that for Pr³⁺ in the borate glass, where it is 4800 cm^{-1} .¹ In the latter glass the UV luminescence efficiency at room temperature is $\sim 60\%$ of the luminescence at 4.2 K. This was partly due to interconfigurational decay to the levels of the $4f^n$ configuration, resulting in a $^1\text{D}_2$ emission. In the Pr³⁺ emission spectrum of the LLP glass at room temperature, no $4f^n$ emission transitions were observed.

This, the smaller Stokes shift, and the absence of temperature dependence of the UV emission intensity lead us to conclude that this UV luminescence of Pr³⁺ in LLP glass is very efficient. This is due to the smaller relaxation of the excited $4f5d$ state of Pr³⁺ in the LLP glass.

Tb³⁺ Ion. The Tb³⁺ ion in LLP glass shows efficient $^5\text{D}_4 \rightarrow ^7\text{F}_J$ emission within the $4f^3$ configuration upon excitation into the $4f^75d$ configuration, which is situated at 225 nm (Figure 5). The excitation spectrum also contains the well-known Tb³⁺ lines. These transitions are orders of magnitude weaker and thus were not studied in detail.

(24) Voropai, E. S.; Gorbachev, S. M.; Saechnikov, V. A.; Cherenda, N. G. *Opt. Spektros. (USSR)* 1987, 62, 1320.

(25) van Die, A.; Blasse, G.; van der Weg, W. F. *Mater. Chem. Phys.* 1986, 14, 513.

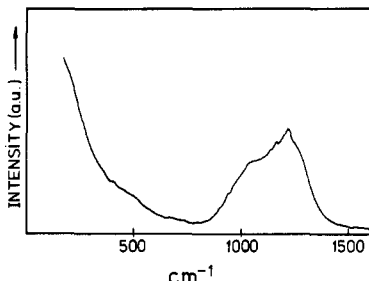


Figure 6. Vibronic side band of the $P_{7/2} \rightarrow S_{7/2}$ emission at 293 K relative to the position of the electronic transition. Excitation wavelength is 278 nm.

The intensity of the $4f^75d$ excitation band implies that the $4f^75d$ configuration feeds the excited levels of the $4f^8$ configuration efficiently. The $7F_J$ levels are obviously not fed. In view of the results discussed above, it is to be expected that the relaxation of the $4f^75d$ configuration is restricted and the configuration coordinate model of Figure 2a is valid for Tb^{3+} in LLP glass if "CTS" is replaced by " $4f^75d$ ". As was shown before,¹ the CTS of Eu^{3+} has a larger relaxation than the $4f^75d$ configuration of Tb^{3+} .

$^{4f^7}$ Excitation of the Gd^{3+} Ion. The luminescence of the Gd^{3+} ion in LLP glass was investigated as this ion has excellent properties as a spectroscopic probe. These properties arise from the presence of a single ground state and a large energy gap of around $32\,000\text{ cm}^{-1}$ between this ground state and the first excited level. After excitation in the 6I_J or 6D_J levels, the Gd^{3+} ion in LLP glass shows a strong emission line at 311.9 nm ($^6P_{7/2} \rightarrow ^8S_{7/2}$), a weaker one at 306 nm ($^6P_{5/2} \rightarrow ^8S_{7/2}$), and a weak vibronic side band from 314 to 326 nm . The decay time of the Gd^{3+} luminescence in LLP glass is $\sim 4\text{ ms}$.

Using narrow-band laser excitation, we observed this vibronic side band in more detail (Figure 6). The strongest vibronic peak is at $\sim 1250\text{-cm}^{-1}$ lower energy than the zero-phonon line. Peaks with lower intensity are at 450 and 1060 cm^{-1} . Our results are in accordance with earlier work on $La(PO_3)_3$: Gd glasses.²⁶ The lower frequency is assigned to a P-O bending vibration, and the higher two to P-O stretching vibrations.²⁷ All vibronic lines are of the cooperative type. The intensity of the vibronic transitions was $\sim 2\%$ of the total emission intensity.

Luminescence of Cr^{3+} . For a long time lithium lanthanum phosphate glass has been reported as the glass with the highest luminescence efficiency for the $^4T_2 \rightarrow ^4A_2$ emission of Cr^{3+} . The quantum efficiency of this broad-band transition in LLP glass is estimated to be 22%.²⁸

Recently, a similar efficiency has been reported for this transition in a germanate glass.²⁹ These germanate glasses are situated in the critical crystallization region and are difficult to produce with a high degree of transparency. The LLP glasses are highly transparent and easy to anneal. The LLP glass seems also more suitable for a comparison with lanthanum borate glass because the former has an absorption edge of almost the same energy as the latter. The quantum efficiency of the LLP: Cr^{3+} glass is much higher than that of the Cr^{3+} -doped lanthanum borate glass, which has a quantum efficiency of $\sim 1\%$ at room temperature. The efficiency of the Cr^{3+} luminescence in LLP glass follows the trend observed for the rare-earth ions.

(26) Hall, D. W.; Brewer, S. A.; Weber, M. *J. Phys. Rev.* 1982, B25, 2828.

(27) Blasse, G.; Brixner, L. H. *Eur. J. Solid State Inorg. Chem.* 1989, 26, 367.

(28) Reisfeld, R.; Jørgensen, C. K. *Struct. Bonding*, 1988, 69, 69.

(29) van Die, A.; Leenaers, A. C. H. I.; Blasse, G.; van der Weg, W. F. *J. Non-Crystalline Solids* 1988, 99, 32.

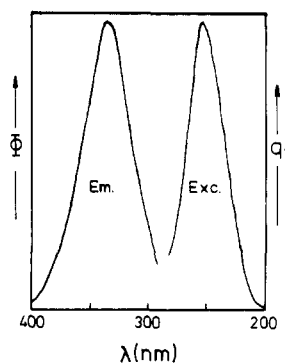


Figure 7. Emission and excitation spectrum of Bi^{3+} luminescence in LLP glass at 4.2 K. The excitation wavelength is 250 nm. The monitored emission wavelength is 360 nm.

Luminescence of Uranyl. The emission spectrum of UO_2^{2+} in LLP consists of a broad band with a pronounced vibrational structure. In the lanthanum borate glass no vibrational structure is observed, not even at 4.2 K.

The uranyl emission in LLP glass is at a higher energy than that in the lanthanum borate glass. Emission peaks are located at 498 , 518 , 542 , and 563 nm , i.e., the peaks are separated by 775 cm^{-1} (the UO_2^{2+} stretching vibration). The peak at 518 nm is the strongest in intensity. In the borate glass the maximum of the emission band was situated at around 550 nm . The emission intensity of the LLP glass starts to decrease around 100 K and drops to 25% at room temperature. For the borate glass these numbers are 50 K and 5% , respectively. These data directly show that the relaxation of the excited state is larger in the lanthanum borate glass than in the LLP glass for the following reasons: (1) The LLP glass shows vibrational structure, whereas the borate does not; however, it cannot be excluded that this is (partly) due to the larger inhomogeneous broadening in the borate glass. (2) The most intense vibronic line is the second one in the LLP glass and probably the third for the borate glass in view of the emission maximum. (3) The quenching starts at a lower temperature in the borate glass.

Unfortunately, it is not possible to introduce the linear uranyl ion substitutionally in the corresponding crystalline lattices. In conclusion, the uranyl luminescence in the LLP glass is much more efficient than that in the lanthanum borate glass, in agreement with the results reported above for other ions.

$^1S_0-^3P_1$ Excitation of the Bi^{3+} Ion. For the Bi^{3+} ion in both the LLP glass and the crystalline modification, luminescence is only observed at low temperatures (150 K and below). In the LLP glass at 4.2 K, the excitation spectrum consists of a band with a maximum at 250 nm. The emission consists of a broad band with a maximum at $\sim 340\text{ nm}$. The Stokes shift is a little more than $10\,000\text{ cm}^{-1}$ (Figure 7), which is almost equal to the value observed for Bi^{3+} in the lanthanum borate glass.¹

In the crystalline modification two types of luminescent Bi^{3+} ions are present. The excitation maxima are 235 and 250 nm and the emission maxima are at 410 and 445 nm, respectively.⁴ The Stokes shift in the crystal is about 1.5 times the Stokes shift in the glass. The Bi^{3+} ion in LLP is the only ion for which the Stokes shift is larger in the crystal than in the glass modification. As we are aware, this is the only example of this phenomenon.

Discussion and Conclusions

From this study it is possible to observe the difference between the luminescence efficiency of a given ion in LLP glass, lanthanum borate glass and the corresponding

Table IV. Luminescence Properties of Activator Ions in Lanthanum Borate and LLP Glass for Excitation in the Broad Excitation Band

	lanthanum borate glass			LLP glass		
	Stokes shift, 10^3 cm^{-1}	max of the exc band, 10^3 cm^{-1}	quantum efficiency at 300 K	Stokes shift, 10^3 cm^{-1}	max of the exc band, 10^3 cm^{-1}	quantum efficiency at 300 K
Eu^{3+}		40.8	very low		50	low
Ce^{3+}	4.7	30.7	high	3.6	34.7	high
Pr^{3+}	4.8	41	high	2.8	45.3	high
Tb^{3+}		42.5	high		44.5	high
Bi^{3+}	10	33.3	very low	10	40	very low
Cr^{3+}	5	~17	very low	4.5 ^a	~15.5	low

^a Reference 31.

crystalline materials. These observations however, have a general bearing.

(a) In the LLP glass the activator ions have a higher luminescence efficiency upon broad-band excitation than in the lanthanum borate glass; however, this efficiency is still low compared to the efficiency of the activator ions in crystals of the same chemical composition. Nevertheless, the LLP glass is a very promising glass host for the efficient luminescence of ions that are excited in a broad absorption band.

(b) The excited state parabolas of these ions in the LLP glass are situated at a higher energy than that in the borate glass, and the Stokes shift of the emission transitions, as far as these can be observed, is smaller than that in the borate glass. There is ample evidence that the relaxation of the excited states increases in the sequence crystals < LLP glass < lanthanum borate glass.

Table IV summarizes the data for both glasses. These data confirm the trends noted before:¹

(a) Ions with broad excitation bands at a high energy and a small relaxation in the corresponding excited state (Ce^{3+} , Pr^{3+} , Tb^{3+}) show efficient luminescence.

(b) Ions with broad excitation bands at a low energy show a low luminescence efficiency (Cr^{3+} , uranyl). The Stokes shift of these ions is smaller in the LLP glass than it is in the borate glass. The efficiency is higher, but it is very low when compared with the efficiency in several crystalline materials.

(c) For comparable situations the relaxation of the excited state in glass is larger than that in the crystalline modification. This is observed for Ce^{3+} , Pr^{3+} , Eu^{3+} , and Tb^{3+} in the LaB_3O_6 crystals and lanthanum borate glass¹ and in the $\text{LiLaP}_4\text{O}_{12}$ crystals and LLP glass. For Eu^{3+} this leads to low efficiencies in the glasses. The larger relaxation in the glass modification has been ascribed to its loose structure³⁰ and the freedom of the ion to choose

its own coordination.³¹ This is even more the case in the borate glass than in the LLP glass. The larger inhomogeneous broadening in the former may be related to this phenomenon. While the phosphate glass contains phosphate tetrahedra, the borate glass may contain borate triangles and tetrahedra.

The Bi^{3+} ion forms an exception to the general rule. Its smaller Stokes shift in the LLP glass when compared to that in the crystalline modification is especially striking. However, in crystalline solids this ion shows a very complicated behavior as discussed at length elsewhere.³⁰ The large Stokes shift in the crystalline modification of LLP has to be ascribed to the off-center Bi^{3+} in the ground state. This off-center position is related to the lone-pair electron configuration of the Bi^{3+} ion ($6s^2$). It is possible to describe this as a pseudo-Jahn-Teller effect due to the mixing of the $^1\text{A}_{1g}$ ground state with the $^1\text{T}_{1u}$ excited state by the t_{1u} (ν_3 , ν_4) vibrational mode.³² Our results seem to suggest that this effect is quenched in the glass, which may be due to the low site symmetry.

Therefore, we come to the following conclusions: (a) For ions with broad-band excitation, efficient luminescence in glasses is possible if the energy difference between the excited state and the ground state is large and the relaxation of the excited state is small. (b) In all other cases (excited state at low energy and/or large relaxation of the excited state) the efficiency of the broad-band excited emission is low, even if it is high in the corresponding crystalline modification.

Acknowledgment. We thank F. A. van Dorsten for his assistance in the preparation of the glasses and the optical measurements.

(31) Imbusch, G. F.; Glynn, T. J.; Morgan, G. P. *J. Lumin.* 1990, 45, 63.

(32) Bersuker, I. B. *The Jahn-Teller effect and vibronic interactions in modern chemistry*; Plenum Press: New York, 1984.